Thermal inversion analysis in Andorra Central Valley and its relationship with pollutants and meteorological variables

L. Trapero[1], A. Crespillo [2], A. Albalat [1], M. Udina [2]

[1] Andorra Research + Innovation, (AR+I), Sant Julià de Lòria, Andorra
[2] Department of Applied Physics - Meteorology, University of Barcelona, Barcelona, Spain

The authors wish to thanks the Air Quality Department of the Government of Andorra for providing the air quality dataset.

Introduction

Figure 1: The study area is located in the north-east of the Iberian Peninsula. Winter image (12/01/2021) of the central valley of Andorra where the orographic complexity and the degree of urbanization can be identified.

The behavior of pollutants in urbanized mountainous areas is complex not only for the interactions between the atmosphere and the orography, also the dynamics of the local and remote sources of emission. The stable Mountain Boundary Layer, present during winter anticyclonic situations favours frequent thermal inversions inside the valley, leading to critical air pollution episodes that are detrimental to human health and the environment.

This study aims to characterize the thermal inversion episodes in a complex orography area like the Andorra Central Valley – ACV (5 km long, 0.5 km wide; Fig.1) during a 18-year period, answering questions like:

(i) Which are the frequency and duration of winter inversion episodes in the central Valley of Andorra?

(ii) How do the winter inversion episodes characteristics correlate with pollutant concentrations and meteorological variables?

Data and methodology

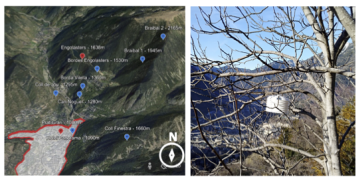

Figure 2: a) Locations of the ground-base stations in ACV: weather and air-quality (red), low-cost sensor (blue).
b) Low-cost sensor installed in Coll de Jou (1298 m).

OBSERVATIONAL DATA (Fig.2)

- **2 automatic weather stations AWS** along ACV: Prat Gran-PG (1080 m) & Engolasters-E (1637 m); [2005-2023 period]
- **1 air-quality station**: Prat Gran (1080 m asl); [2005-2023 period]; Pollutants: NO_2, PM_{10} and O_3
- **8 low-cost sensors** temperature and humidity; [2020-2023 period]

METHODOLOGY (Beaufils, 2021)

→ **Thermal inversion characterization** frequency, duration and inversion strength (IST; ºC/km)

Detection based on the gradient of 2 AWS
$\Delta T = T_{2m}(E) - T_{2m}(PG) > 0ºC$ (1)

$$IST = \frac{1}{n}\sum_{i=1}^{n}\frac{(T_{2mE} - T_{2mPG})}{(Alt_E - Alt_{PG})} \times 1000 \quad (2)$$

→ Relationship between thermal inversions (>6h) and pollutants

→ Explore the use of low-cost sensors to monitor thermal inversions (pseudo-profiles)

Results and conclusions

Thermal inversion characterization

a) Frequency: 1139 thermal inversion episodes (>1h) in 18-years, mostly occurring during the cold season (Nov-Mar) and mainly starting before the sunrise (8-9h). 2022 is the year with most episodes (108).

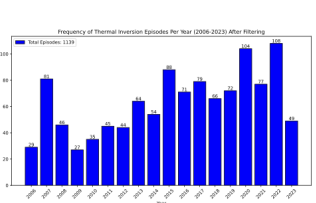

Figure 3: Number of inversion episodes (>1h) detected over the 18-year period.

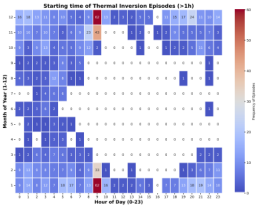

Figure 4: Heat map showing the monthly frequency of the starting hour of the inversion episodes (>1h)

b) Duration:
62% of the episodes lasting less than 6h;
37% of the episodes have a duration greater than 6h (**diurnal inversion**) & only 22 episodes (2%) could be considered as **persistent thermal inversions** – PTI (>24h)

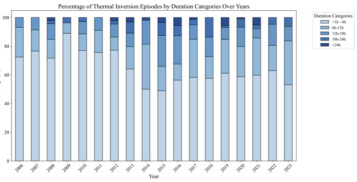

Figure 5: Occurrence (%) over the years of the episodes of thermal inversion according to their range of duration in hours. Categories: 1-6h, 6-12h, 12-18h, 18-24h and >24h.

c) IST- Inversion Strength:
Despite no trends in IST are detected along the 18-year period, occasional outliers seems to be more frequent in the last 5-years. Seasonality is detected in the magnitude of the IST: higher in the winter months than in the summer.

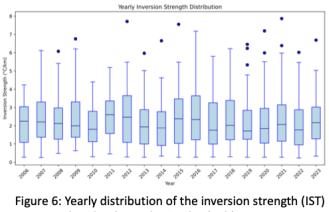

Figure 6: Yearly distribution of the inversion strength (IST) associated to the thermal episodes (>6h).

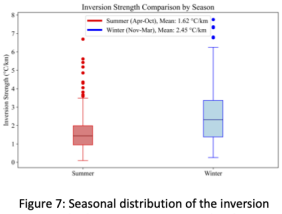

Figure 7: Seasonal distribution of the inversion strength (IST) for thermal episodes (>6h).

d) Duration (hours) vs IST (ºC/km) :
Moderate positive correlation is detected (0.53 Pearson coefficient), implying that as the inversion strength increases, so does the probability of longer-duration thermal episodes.

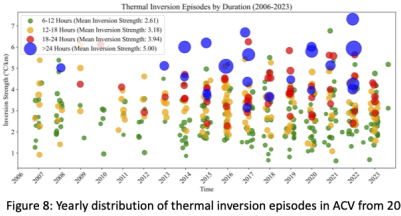

Figure 8: Yearly distribution of thermal inversion episodes in ACV from 2006 to Sept 2023 based on their associated IST (ºC/km) and their duration (h).

Meteorology & Pseudo-Profiles

Meteorological overview and air pollutants evolution during the longest persistent thermal inversion episode 1 (PTI-E1), from 2021/12/29 23:00 to 2022/01/03 08:45, lasting more than 4 days.

The main persistent inversions (PTI) occur during high-pressure conditions, initially forming a synoptic-scale elevated inversion due to the advection of warm air masses in the mid-troposphere. The inversion break-up occurs rapidly when at synoptic scale cold air is advected (Largeron & Staquet, 2016). PTI-E1 mainly induced a PM_{10} episode and exacerbated NO_2 episode.

PTI-E1: 2021/12/29 to 2022/01/03

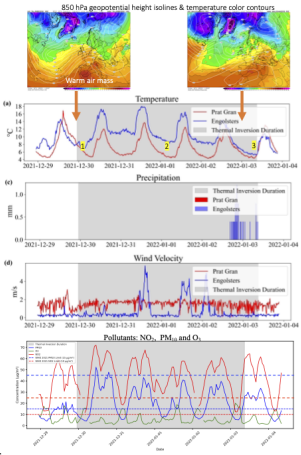

Vertical temperature PSEUDO-PROFILES

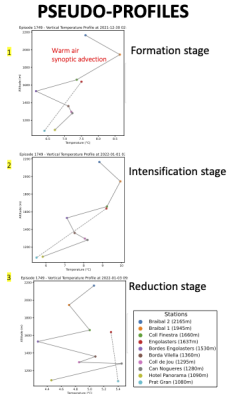

Effectiveness of low-cost sensors is notably dependent on their placement (altitude and orientation).

Pollutant concentration analysis

Findings in Lemus et al. (2019) indicate an increasing frequency of winter synoptic high-pressure conditions in Andorra conducive of thermal inversion episodes and air pollutant episodes. The results (Fig. 9 and 10) show that thermal inversions episodes significantly contribute to NO_2 and PM_{10} episodes, nearly doubling their average levels. Despite O_3 maxima did not show a correlation with thermal inversion, during warm months, exceedances of critical thresholds have increased during last decades.

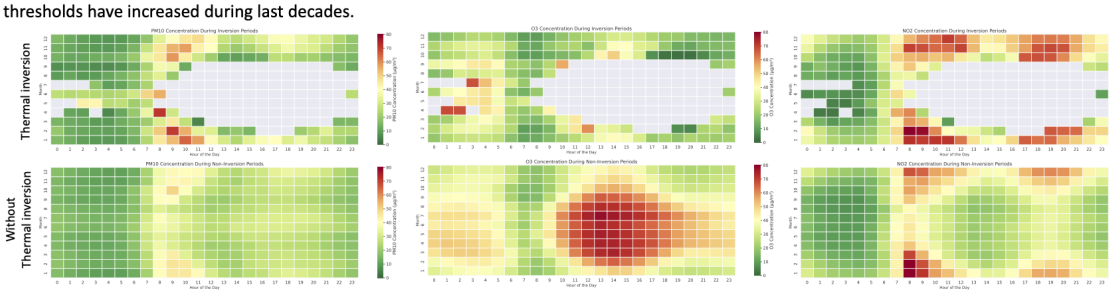

Figure 9: Heat map showing the mean hourly levels of pollutants concentration (PM_{10}, O_3 and NO_2) at monthly scale during both: thermal inversion episodes and non-inversion situations.

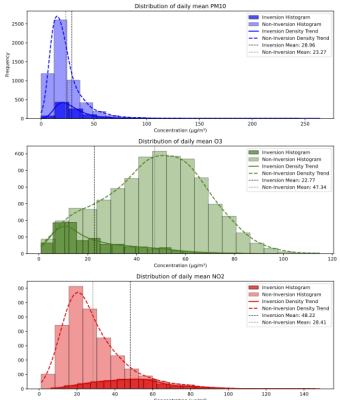

Figure 10: Histograms comparing daily mean levels of pollutants concentrations (PM_{10}, O_3 and NO_2) during both: thermal inversion episodes and non-inversion situations.

References:
Beaufils, S., IEENM3/ENM (2021). Wintertime mountain boundary layer in the central valley of andorra: temperature inversion and air quality.
Largeron, Y., and C. Staquet (2016). Persistent inversion dynamics and wintertime PM10 air pollution in alpine valleys, Atmospheric Environment, 135, 92–108, doi:10.1016/j.atmosenv.2016.03.045.
Lemus-Canovas, M., Ninyerola, M., Lopez-Bustins, J. A., Manguan, S., & Garcia-Sellés, C. (2019). A mixed application of an objective synoptic classification and spatial regression models for deriving winter precipitation regimes in the Eastern Pyrenees. International Journal of Climatology, 39(4), 2244–2259. https://doi.org/10.1002/joc.5948